Chemistry and Physics of Lipids 165 (2012) 142–150

Contents lists available at SciVerse ScienceDirect

Chemistry and Physics of Lipids

journal homepage: www.elsevier.com/locate/chemphyslip

Differing modes of interaction between monomeric $A\beta_{1-40}$ peptides and model lipid membranes: an AFM study

Khizar Sheikh[a,*,1,2], Cristiano Giordani[a,1,3], Jennifer J. McManus[b], Mads Bruun Hovgaard[a], Suzanne P. Jarvis[a]

[a] Nanoscale Function Group, Conway Institute of Biomolecular and Biomedical Research, University College Dublin, Belfield, Dublin 4, Ireland
[b] Department of Chemistry, National University of Ireland Maynooth, Maynooth, Co. Kildare, Ireland

ARTICLE INFO

Article history:
Received 22 September 2011
Received in revised form
24 November 2011
Accepted 25 November 2011
Available online 9 December 2011

Keywords:
β-Amyloid peptide
Atomic force microscopy
Model phospholipid membranes
DOPC
DPPC
Cholesterol

ABSTRACT

Membrane interactions with β-amyloid peptides are implicated in the pathology of Alzheimer's disease and cholesterol has been shown to be key modulator of this interaction, yet little is known about the mechanism of this interaction. Using atomic force microscopy, we investigated the interaction of monomeric $A\beta_{1-40}$ peptides with planar mica-supported bilayers composed of DOPC and DPPC containing varying concentrations of cholesterol. We show that below the bilayer melting temperature, Aβ monomers adsorb to, and assemble on, the surface of DPPC bilayers to form layers that grow laterally and normal to the bilayer plane. Above the bilayer melting temperature, we observe protofibril formation. In contrast, in DOPC bilayers, Aβ monomers exhibit a detergent-like action, forming defects in the bilayer structure. The kinetics of both modes of interaction significantly increases with increasing membrane cholesterol content. We conclude that the mode and rate of the interaction of Aβ monomers with lipid bilayers are strongly dependent on lipid composition, phase state and cholesterol content.

1. Introduction

Neurodegenerative Alzheimer's disease (AD) is characterized by the presence of extracellular senile plaques of which the main protein constituent is β-amyloid (Aβ) peptides (Selkoe, 1991; Irvine et al., 2008). The peptides are generated by cleavage of membrane-bound amyloid precursor protein by proteases and vary in length between 38 and 42 residues, with the 40 and 42 residue peptides being the most common isoforms associated with amyloid plaques (Haass et al., 1992; Hartmann et al., 1997). Neurotoxicity is associated with isoforms containing the β29–35 region and studies have shown that both soluble oligomers and insoluble mature fibrils (but not the soluble monomers) are neurotoxic (Pike et al., 1993; Walsh et al., 1997, 1999, 2002). A body of evidence has also accumulated showing that Aβ preparations interact with both model membranes and cells to form cationic selective ion channels. Associated with this is an increase in cytosolic calcium levels and cell degradation (Arispe et al., 1993a,b; Bhatia et al., 2000; Demuro et al., 2005; Kawahara et al., 1997; Lin et al., 1999; Nag et al., 2010). The differing Aβ preparation methods employed in many cases makes it difficult to assign the observed effects to a particular Aβ aggregation state.

Whilst cellular membrane studies may be considered to be more physiologically relevant, the use of model membranes allows the study of Aβ interactions with membranes of controlled composition. The nanometer scale imaging resolution afforded by atomic force microscopy (AFM) is particularly well suited to the study of planar membrane interactions with small peptides such as Aβ. A previous AFM study of the interaction of $A\beta_{1-42}$ deposited onto phase separated mica-supported membranes composed of DOPC and DPPC showed Aβ aggregation onto the DPPC phase but not the DOPC phase (Choucair et al., 2007). Another AFM study of $A\beta_{1-40}$ deposited onto mica-supported membranes composed of total brain lipid extracts and also onto DMPC membranes showed membrane disruption via fibril growth (Yip and McLaurin, 2001). Other AFM studies have shown the formation of pore-like structures in supported DOPC bilayers formed from Aβ peptides pre-sonicated with lipid vesicles (Quist et al., 2005).

The origin of the discrepancies between AFM studies is uncertain, but again, differing Aβ preparation methods employed makes

Abbreviations: Aβ, β-amyloid peptide; DOPC, 1,2-Dioleoyl-*sn*-glycero-3-phosphocholine; DPPC, 1,2-Dipalmitoyl-sn-glycero-3-phosphocholine; AFM, atomic force microscopy; AM, amplitude modulation; FM, frequency modulation; QLS, quasielastic light scattering.

* Corresponding author. Tel.: +353 1 716 6762; fax: +353 1 716 6777.
E-mail addresses: khizar_001@yahoo.co.uk (K. Sheikh), suzi.jarvis@ucd.ie (S.P. Jarvis).
[1] These authors contributed equally to this work.
[2] Permanent address: 164 Redesdale Gardens, Leeds LS16 6AX, UK.
[3] Permanent address: Via Iglesias 7, 00182 Roma, Italia.

0009-3084/$ – see front matter © 2011 Elsevier Ireland Ltd. All rights reserved.
doi:10.1016/j.chemphyslip.2011.11.011

it difficult to assign the observed effects to a particular Aβ aggregation state.

Cholesterol has been shown to play a key role in the pathogenesis of Alzheimer's disease, with experiments showing that cholesterol both directly interacts with Aβ and also modulates the activity of β and γ secretase enzymes (Avdulov et al., 1997; Bodovitz and Klein, 1996; Harris, 2008; Shobab et al., 2005; Wahrle et al., 2002). In an AFM study, exogenous cholesterol enhancement of total brain lipid extract increased membrane disruption whereas cholesterol depletion by methyl-β-cyclodextrin eliminated membrane association with $A\beta_{1-40}$ (Yip et al., 2002).

In order to gain insight into the mechanism of the Aβ-membrane interaction, we investigate the interaction between $A\beta_{1-40}$ monomers and mica-supported membranes composed of the saturated lipid DPPC and the unsaturated lipid DOPC whilst systematically varying the membrane cholesterol content. We employed HPLC isolated monomers fractions of $A\beta_{1-40}$ in order to assign any observed membrane interactions to this aggregation state.

We opted to use $A\beta_{1-40}$ rather than $A\beta_{1-42}$ as its lower rate of fibrillation would be more amenable to study by the relatively slow (ca. 4 min/frame) AFM imaging technique.[6] We employed zwitterionic lipids for this study as they were shown not to significantly alter the predominantly random coil structure of low molecular weight (LMW) Aβ solutions, unlike anionic lipids which can induce the formation of β-sheet structures (Terzi et al., 1995; McLaurin and Chakrabartty, 1997; Snyder et al., 1994).

We show that the associative interaction of $A\beta_{1-40}$ monomers with DPPC bilayers is dependent on the phase state of the bilayer and see a significant increase in the kinetics of association with increasing membrane cholesterol content. In DOPC bilayers we see extensive disruption of the membrane structure by $A\beta_{1-40}$, the rate of which drastically increases with increasing membrane cholesterol content. The results have widespread implications for Aβ interactions with membrane systems, such as lipid rafts, which contain high proportions of saturated lipids and cholesterol.

2. Materials and methods

2.1. Isolation of Aβ monomers

Synthesized and purified $A\beta_{1-40}$ was purchased as a lyophilized powder from Dr. James I. Elliott at Yale University (New Haven, CT) and stored at −80 °C before use. To prepare Aβ monomers, the dried powder was dissolved in an equal mixture of 0.1% NH_3OH and 100 mM Tris–HCl, pH 8.0, and then diluted to the required concentration (usually 2 mg/ml) by the addition of sodium phosphate buffer (pH 7.0) to give a final sodium phosphate concentration of 10 mM. The solution was then centrifuged at 15,000 rpm for 1.5 h. Quasielastic light scattering of these samples was performed on an ALV CGS 3 compact goniometer system (ALV GmbH), with a scattering angle of 90°. This was to ensure that no large aggregates were present in the sample. The monomeric peptide was then isolated by HPLC (Shimadzu), equipped with an autosampler, diode array detector and fraction collector. Separation was performed using a 5/150 Superdex 75 column (GE Healthcare) using 10 mM sodium buffer as the mobile phase and a flow rate of 0.3 ml/min. The protein was detected at 280 nm. The fraction containing peptide monomers was collected and the concentration of the sample was determined by UV–visible absorbance using a molar extinction coefficient of 1490 cm^{-1} M^{-1}. Samples were snap-frozen immediately after concentration determination. Samples were defrosted and filtered through 20 nm Anatop filters (Whatman) immediately before AFM experiments. Aβ monomers were added into the lipid bilayer at concentrations ranging from 4 to 9 μM.

2.2. Lipid bilayer preparation

Synthetic 1,2-Dipalmitoyl-sn-glycero-3-phosphocholine (DPPC), 1,2-Dioleoyl-*sn*-glycero-3-phosphocholine (DOPC) and cholesterol were purchased from Sigma–Aldrich. Solutions of DPPC, DOPC and cholesterol were prepared in chloroform to concentrations of 5 mM. Appropriate volumes of lipids and cholesterol solutions were vortexed in a glass vial under Argon gas and dried under an Argon gas flow. The sample was then placed in a vacuum desiccator for at least 40 min to remove solvent traces. Sodium phosphate pH 7.0 buffer solution was added to give a final sample concentration of 1 mg ml^{-1} and the sample vortexed at 1400 rpm at room temperature (DOPC) or 50 °C (DPPC) for 30 min to hydrate and disperse the lipid film. Unilamellar vesicles were obtained by the extrusion method. The solution of hydrated lipid multilayer was passed through a nucleopore polycarbonate membrane with 50 nm mean pore diameter 11 times, yielding a solution of unilamellar vesicles of uniform size, using a miniextruder system (Avanti Polar Lipids). High-grade V-1 muscovite mica discs (SPI supplies) were glued onto a Teflon disc (Supelco) mounted on a glass slide and cleaved with adhesive tape immediately before use. Supported bilayer were formed on the mica substrates using the vesicle fusion method where 100 μl of lipid vesicles solution was immediately deposited onto the freshly cleaved mica surface and incubated at room temperature (DOPC) or 50 °C (DPPC) for 30 min and 2 h, respectively. The vesicles solution was rinsed by fluid exchange seven times with fresh buffer before the substrate holder was placed in the AFM for imaging.

2.2.1. AFM imaging

The AFM measurements were performed using an MFP-3D-SA AFM (Asylum Research, Santa Barbara, CA) operated in amplitude modulation (AC) mode. SNL cantilevers (Bruker) having nominal spring constants of 0.24 N m^{-1} and nominal tip radii of 2 nm were used for imaging of Aβ samples on mica and of DPPC bilayers. DNP cantilevers (Bruker) having nominal spring constants of 0.32 N m^{-1} and nominal tip radii of 20 nm were used for imaging of DOPC bilayers. Typical AC mode AFM parameters used in the experiments were drive frequencies of 14.5 kHz, free root-mean-square (RMS) cantilever oscillation amplitudes of 500 mV and RMS amplitude imaging setpoints of 300–490 mV, with scan rates of 1–2 Hz.

3. Results

3.1. Aβ size characterization

We employed quasielastic light scattering (QLS) to characterize the size distribution of Aβ aggregates within the suspensions prepared for the experiments and separated Aβ monomers from the suspension using HPLC. A typical fitted output of quasielastic light scattering experiments of a total Aβ suspension is shown if Fig. 1 A. The typical average hydrodynamic radius was 7 nm, consistent with values determined previously using QLS and small angle neutron scattering (SANS) (Walsh et al., 1999; Yong et al., 2002). This represents a polydisperse mixture of Aβ monomers and small (LMW) oligomers. The hydrodynamic radius of the Aβ monomers was determined to be 1.5 nm (Fig. 1A). The contribution to the QLS scattering intensity from even small amounts of LMW oligomers (with larger hydrodynamic radii) can result in small increases in the hydrodynamic radius determined for the monomer. The HPLC elution profile in Fig. 1B indicates effective separation of Aβ monomers from the higher order oligomers. Monomeric Aβ solution (after snap-freezing and thawing, post HPLC) was deposited on mica and imaged in phosphate buffer as shown in Fig. 1C. Features having globular morphology can be seen with a height distribution of

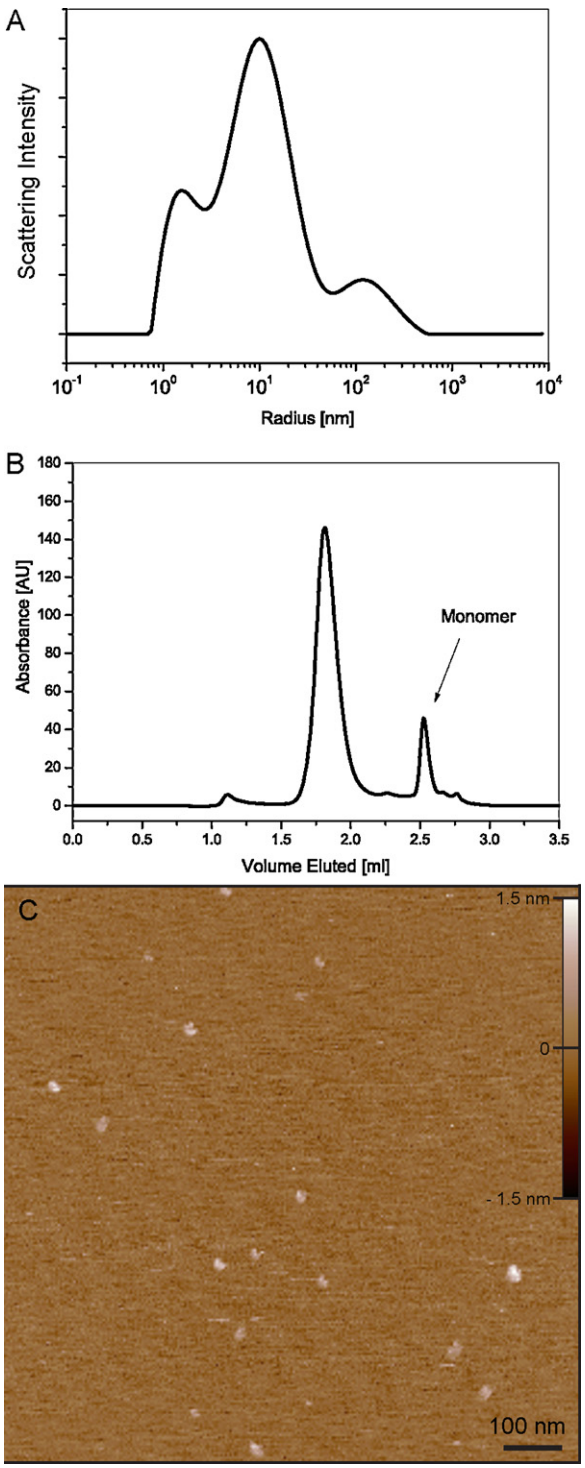

Fig. 1. (A) Graph showing the distribution of hydrodynamic radii of the total Aβ mixture before HPLC as determined by quasielastic light scattering. (B) Typical chromatograph obtained in the separation of Aβ monomers from higher molecular weight oligomers using HPLC prior to AFM experiments (C) AFM height image of the HPLC-isolated Aβ monomers deposited on a mica substrate and imaged in phosphate buffer.

1 ± 0.2 nm and diameters of 16.2 ± 3.3 nm. The measured diameters will also be convoluted with the tip radius of the AFM cantilever (nominally 2 nm, maximum 12 nm) and therefore the measured heights are considered to provide a more accurate size indication. The measured heights compare with ca. 2 nm as measured in a previous AFM study of LMW Aβ (Losic et al., 2006). We do not exclude the existence of extremely small proportions of LMW oligomers in the Aβ solutions used, although a previous study of $A\beta_{1-40}$ aggregation has shown a lack of detectable oligomerization at the low Aβ concentrations used in this study (4–9 μM) over the timescales of our measurements (less than 1 h) (Snyder et al., 1994).

3.2. Interactions between Aβ and DPPC bilayers

We initially investigated the effect of Aβ on DPPC bilayers formed on mica substrates. Fig. 2A shows a 10 μm × 10 μm scan of the DPPC bilayer, pre-Aβ incubation, imaged at 26.4 ± 0.1 °C. The bilayer covered 97.8% of the surface area and formed micrometer-sized domains which arise from differing azimuthal tilt directions of the lipid acyl chains forming the domains (Rinia et al., 2000). It should also be noted that DPPC bilayers formed on mica substrates at this temperature show mesoscale positional molecular order associated with being in a pseudocrystalline pre-transition phase (Sheikh et al., 2011). The depth of defects associated with these domain boundaries showed two distributions; the first with a depth of 4.3 ± 0.3 nm and 0.7% surface area coverage assigned to the underlying mica substrate, and the second with a depth of 1.5 ± 0.2 nm and 1.4% surface area coverage attributed to a single lipid monolayer. There is also a small 0.1% surface area coverage of extraneous material of height less than 5 nm. The bilayer thickness is consistent with the saturated DPPC acyl chains of the bilayer being predominantly in an extended *trans* conformation and is also in good agreement with previous AFM and X-ray diffraction studies (Rinia et al., 2000; Sheikh et al., 2011; Yarrow et al., 2005; Sun et al., 1994). Aβ monomers at a concentration of 4 μM were incubated with DPPC bilayers and imaged in phosphate buffer at pH 7 at temperatures varying between 26 and 44 °C with representative images shown in Fig. 2B–D. At a temperature of 26.4 ± 0.1 °C we observed the formation of isolated rounded layers formed by Aβ assembly having a height of 5.5 ± 0.5 nm (above the bilayer surface) and with diameters of ca. 400 nm. The Aβ assemblies formed within 10 min of injection of Aβ into the AFM fluid cell and continuous imaging of the same area over 60 min showed that the height of the assemblies did not vary significantly over this time. The surface area covered by Aβ (as defined by the height of protruding features over 1 nm) increased slowly over this time from 0.26% to 0.68%.

We imaged the Aβ-DPPC interaction at increased temperature. Up to the main chain melting transition temperature (Tm) of the DPPC bilayer (42 °C), we did not observe a significant difference in height or morphology compared to that seen at 26 °C over a period of 60 min. However, within 5 min of Aβ incubation at 44 ± 0.1 °C, we observed the formation of short, curved fibrillar structures (Fig. 2C), the surface coverage of which increased to 1.17% after 45 min (Fig. 2D). The heights of these protofibrillar structures were 4.4 ± 0.4 nm with lengths up to 200 nm. EM studies of $A\beta_{1-40}$ morphology show that oligomerization results in the formation of protofibrils with diameters of 5 nm and lengths of ca. 100 nm, suggesting that the structures seen here are protofibrils (Fraser et al., 1992).

3.3. Interactions between Aβ and DPPC bilayers containing cholesterol

We formed DPPC bilayers incorporating 33 mol% of cholesterol and imaged the time sequence of the interaction with Aβ monomers (at a concentration of 4.6 μM) by continuous scanning of the same areas at 25 ± 1 °C and representative images of the interaction are shown in Fig. 3A–F. We observed that the amyloid monomers aggregated on the surface of the bilayer and grew laterally. We saw a drastic increase in the initial kinetics (within 14 min) of bilayer surface area coverage by Aβ monomers compared to that seen with pure DPPC bilayers, with an increase of two orders of

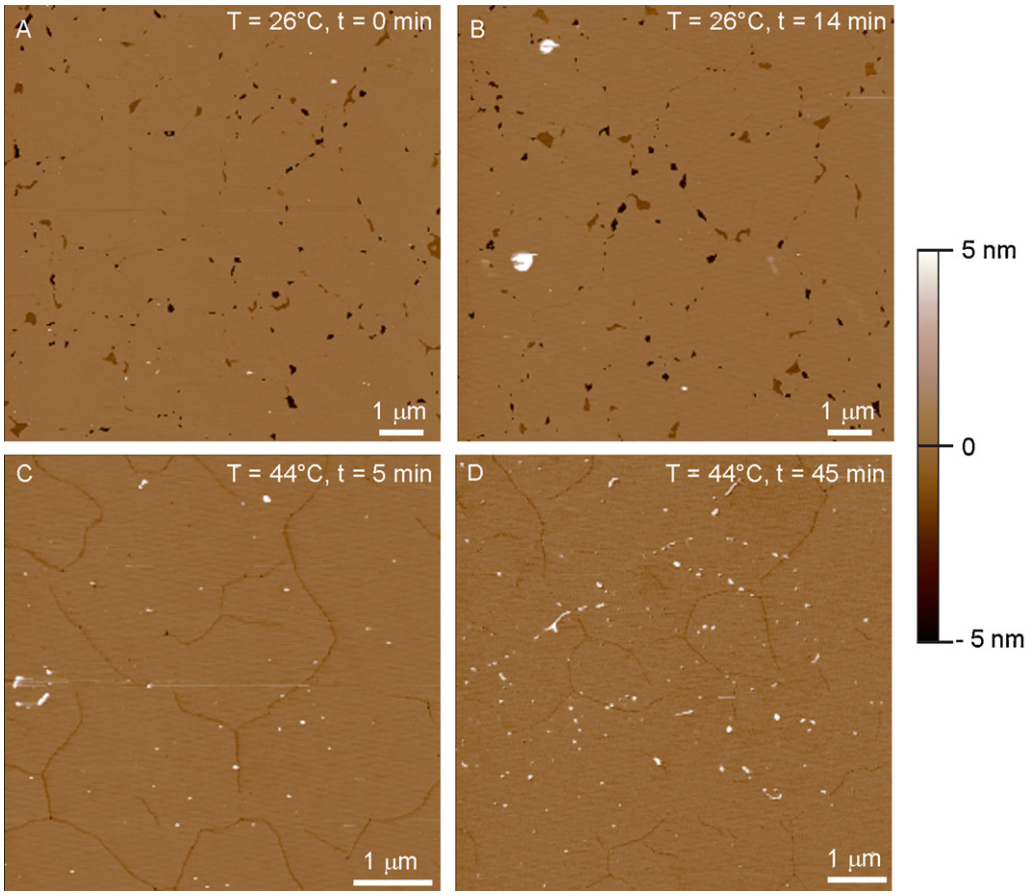

Fig. 2. AFM height images showing adsorption of Aβ monomers on the surface of DPPC bilayers imaged in phosphate buffer. (A) Pre-Aβ incubation, $T = 26\,^{\circ}C$. (B) Post-Aβ incubation, $T = 26\,^{\circ}C$, $t = 14$ min. (C) Post-Aβ incubation, $T = 44\,^{\circ}C$, $t = 5$ min. (D) Post-Aβ incubation, $T = 44\,^{\circ}C$, $t = 45$ min. Below the bilayer melting temperature of 42 °C, the Aβ monomers form isolated, nanometer-sized, rounded assemblies whereas above the bilayer melting temperature, the Aβ monomers form protofibrillar structures.

magnitude (Fig. 3G). It can also been seen from Fig. 3G that the kinetics of subsequent layer formation is also faster. The Aβ layer initially forms with a height of 3.6 ± 0.4 nm above the bilayer surface, suggesting increased incorporation of the Aβ assembly into the headgroup region of the bilayer and an increase in affinity of Aβ with DPPC bilayers in the presence of cholesterol. This is supported by previous studies showing increased bilayer incorporation of Aβ with increasing cholesterol/phospholipid ratio (Gershfeldt, 1978). The thickness of the Aβ layer was also seen to increase with time (Fig. 3H), a phenomenon which was not observed for pure DPPC bilayers over the timescales studied. Incubation of monomeric Aβ (at a concentration of 4.6 μM) with DPPC bilayers having a cholesterol concentration of 50 mol% also resulted in the formation of layered assemblies of Aβ monomers. Again, the initial kinetics of layer formation was rapid, with an initial layer thickness of 3.3 ± 0.4 nm over a surface area of ca. 1.5% forming within 5 min of incubation with Aβ monomers (Fig. 4A). The subsequent area coverage increased more slowly to ca. 1.9% over 40 min probably as a result of depletion of the Aβ solution. At this cholesterol concentration, bilayer defects were observed with depth of ca. 4.5 nm and Aβ monomers were seen to absorb to the mica through these defects. The Aβ layer heights suggest incorporation of the Aβ assembly into the bilayer in the presence of cholesterol. We observed a significant change in the observed height of the Aβ layer with imaging force. Successive scans of the same area (Fig. 4A) showed that with even a small change (ca. 50 pN) of imaging force, the measured bilayer height fell to 0.7 ± 0.4 nm (Fig. 4B). Subsequently lowering the imaging force by the same amount resulted in the bilayer height recovering to approximately the same height (4.9 ± 0.7 nm) (Fig. 4C). We also captured images of the phase response of the AFM cantilever during imaging and these are shown in Fig. 4D–F for the height images shown in Fig. 4A–C. The phase change of the cantilever oscillation during imaging is related to the energy dissipation of the AFM cantilever arising from dissipative tip-sample interactions (Cleveland et al., 1998). Fig. 4D and F shows slightly higher dissipation in regions of the bilayer containing defects where Aβ monomers have adsorbed to the mica substrate as well as regions where Aβ monomers have adsorbed to the lipid bilayer. In comparison, the phase image taken with slightly higher imaging force (Fig. 4B) shows similarly higher dissipation in the defect areas (as a result of the higher imaging force) but *lower* dissipation in the region where the Aβ assembly has incorporated into the bilayer.

3.4. Interactions between Aβ and DOPC bilayers

Lipids forming cellular plasma membranes may contain fatty acid chains that are saturated or unsaturated, with a study of neuronal vesicles showing a membrane composition of predominantly unsaturated fatty acids (Takamori et al., 2006). We therefore performed similar experiments to incubate a model lipid, DOPC (with varying concentrations of cholesterol) with monomeric Aβ to see if any differences arose from differing lipid acyl chain saturation. A previous study using AFM by Choucair et al. (2007) using phase-separated DOPC/DPPC bilayers and a pre-incubated Aβ solution observed an interaction of Aβ with the DPPC phase only.

Being in the fluid phase, the DOPC bilayers (Fig. 5A) appeared relatively featureless and defect free compared to DPPC bilayers due to the higher lateral diffusion coefficients of the lipids molecules.

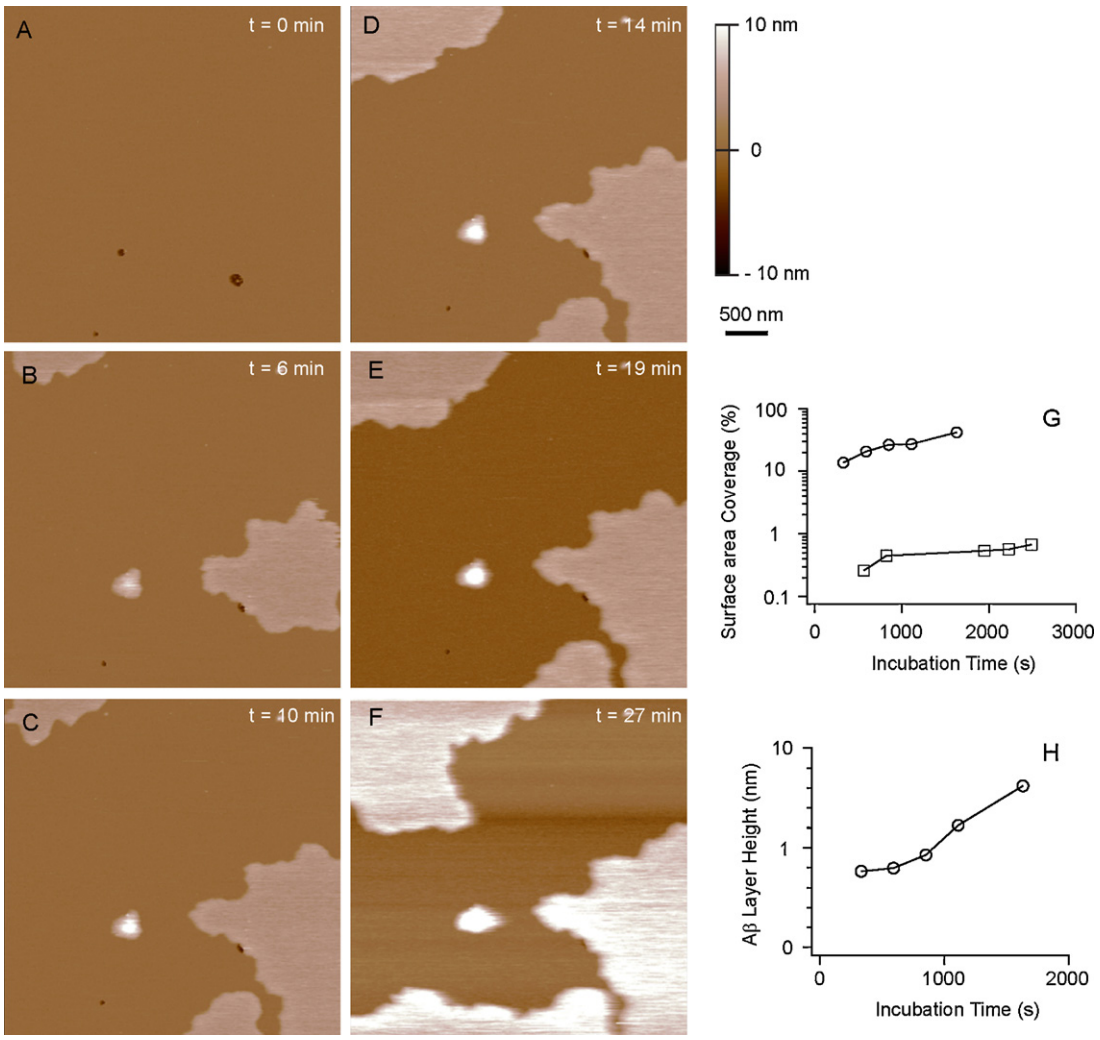

Fig. 3. (A–F) Time sequence AFM height images showing the assembly of Aβ monomers on the surface of a DPPC bilayer containing 33 mol% cholesterol at $T = 25\,^{\circ}C$. The monomers assemble on the bilayer surface to form layered structures that grow both laterally and normal to the bilayer surface. (G) Graph showing the increase in surface area coverage of the Aβ layer over time (□ – DPPC bilayer, ○ – DPPC + 33 mol% cholesterol bilayer). (H) Graph showing the increase in height of the Aβ layer (above the bilayer surface) over time.

Within 10 min of incubation with 6.9 μM Aβ, we saw the formation of defects of around 800 nm in diameter over a bilayer surface area of 0.8% (Fig. 5B). Subsequent defect growth was slower as shown by the images of the same area shown in Fig. 5C and D, taken 90 min apart, probably as a result of Aβ depletion. Higher magnification imaging of the defects, shown in Fig. 5C shows the formation of globular structures within the defects with approximate diameters of 40 nm and heights of up to 10 nm. The diameters are convoluted by tip geometry and are therefore not accurate absolute measurements of size, however as the heights are well above those of the bilayer (4.5 nm) it is evident that a new type of structure was formed, probably composed of both Aβ and lipid. Comparison of the images shown in Fig. 5C and D (of the same defect) 90 min apart show the formation of new globular structures in regions where membrane disruption has occurred. One of these globular structures is indicated in Fig. 5D in a region adjoining the edge of the membrane defect where membrane regression is evident from comparison with Fig. 5C.

3.5. *Interactions between Aβ and DOPC bilayers containing cholesterol*

Increasing the cholesterol content of the DOPC bilayers resulted in an increase in the rate of membrane disruption (Fig. 6). Fig. 6A–C shows images taken 10 min after the incubation of DOPC bilayers containing 10, 25 and 50 mol% cholesterol with 4.6 μM monomeric Aβ where the area of bilayer coverage has decreased to 23, 6 and 0% respectively.

4. Discussion

Comparison of the monomeric hydrodynamic radius of 1.5 nm determined by QLS and the measured AFM height of 1 nm suggests that the monomer height is reduced by the imaging force of the tip (c. 0.5 nN). The mechanical strength of peptides is determined by secondary, supersecondary and tertiary structure. Monomeric Aβ has been shown to have a predominantly random coil structure and measurements of the elastic moduli of peptides with low structural order show low elastic moduli (Walsh et al., 1999; Bitan et al., 2003; Middleburg et al., 2008; Leon et al., 1998). This may be reflected in the height measurements, but as noted previously, small amounts of LMW oligomers (with larger hydrodynamic radii) can result in small increases in the hydrodynamic radius as determined by QLS for the monomer. The monomer size is therefore taken as between these two bounds.

Given the measured monomer size, the heights of the amyloid assembled on DPPC bilayers show the surface adsorption of an

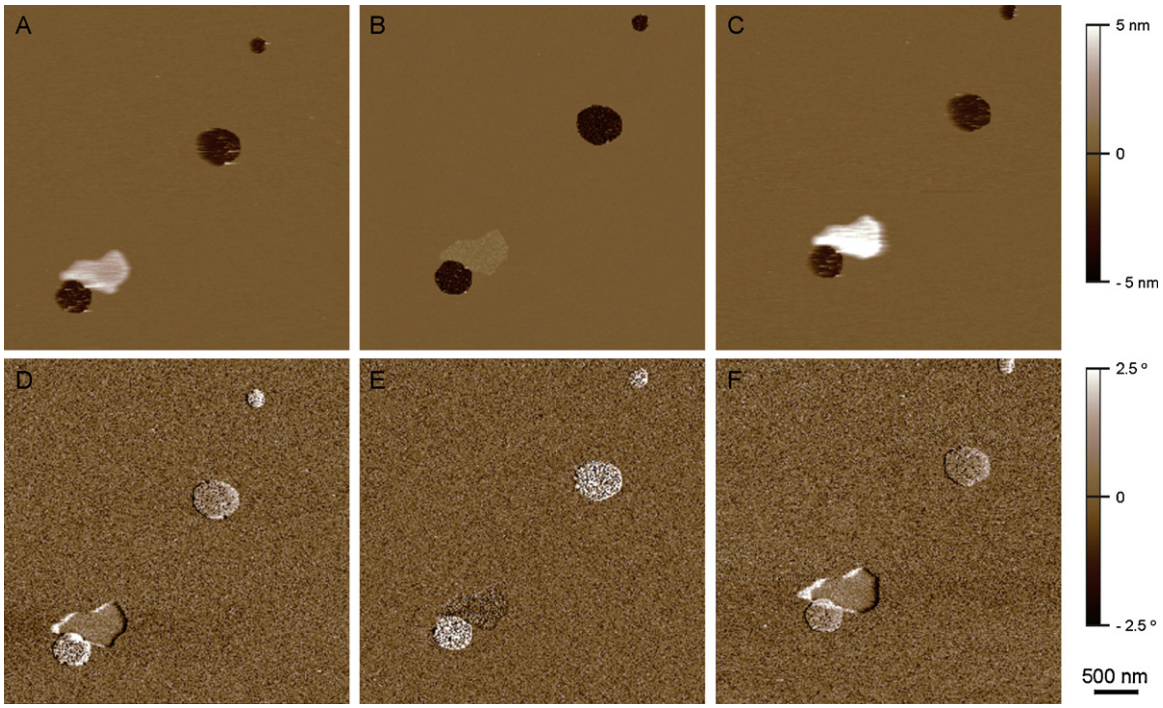

Fig. 4. Sequential AFM height (A–C) and corresponding phase images (D–F) showing the assembly of Aβ monomers onto the surface of a DPPC bilayer (A and D) containing 50 mol% cholesterol to form a layered assembly. Increasing the AFM tip imaging force by 50 pN induces the Aβ assembly to insert into the core of the bilayer (B) to form a structure that was less dissipative than the bilayer itself. Subsequently lowering the AFM tip imaging force by 50 pN results in the Aβ assembly reverting to its position on the surface of the bilayer, indicating that the insertion is reversible.

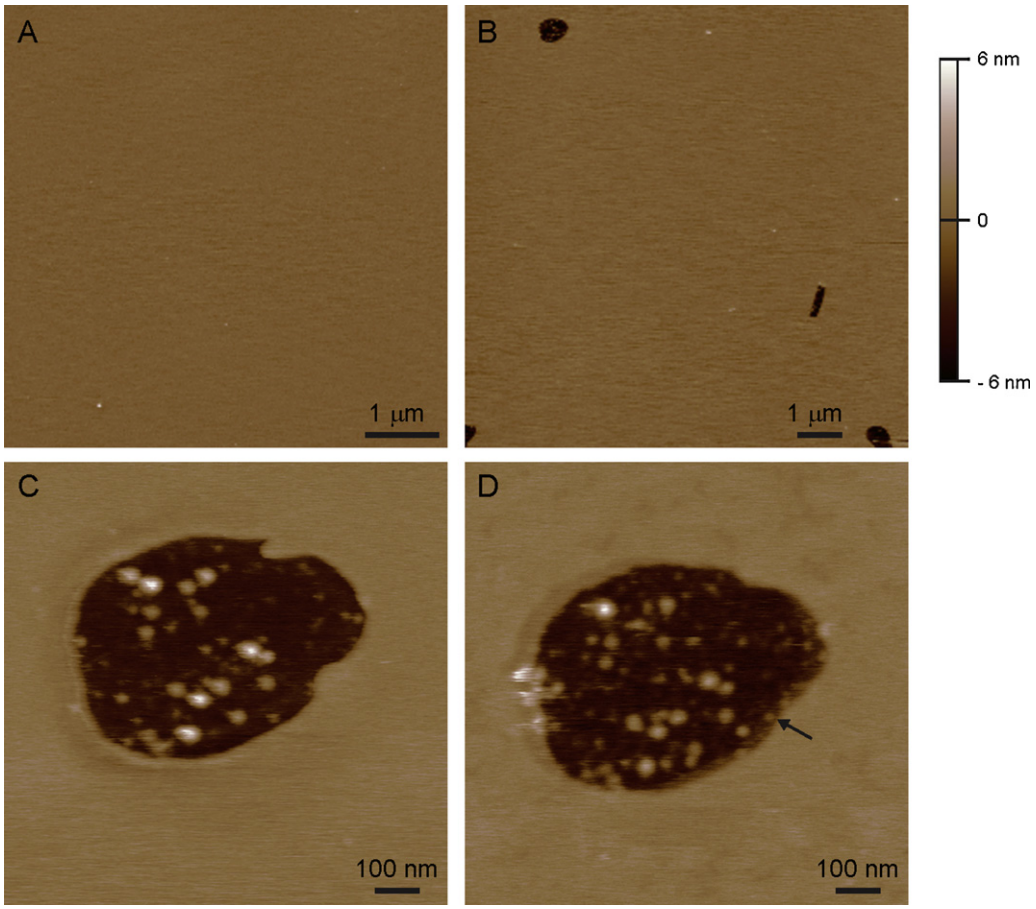

Fig. 5. AFM height images showing the formation of defects in DOPC bilayers arising from incubation with Aβ monomers. (A) Pre-Aβ incubation and (B) post-Aβ incubation, $t = 14$ min. (C and D) Higher resolution sequential images show the formation of globular structures at the growing defect boundary, showing detergent-like solubilization of the unsaturated lipid bilayer by the amphiphilic Aβ peptides.

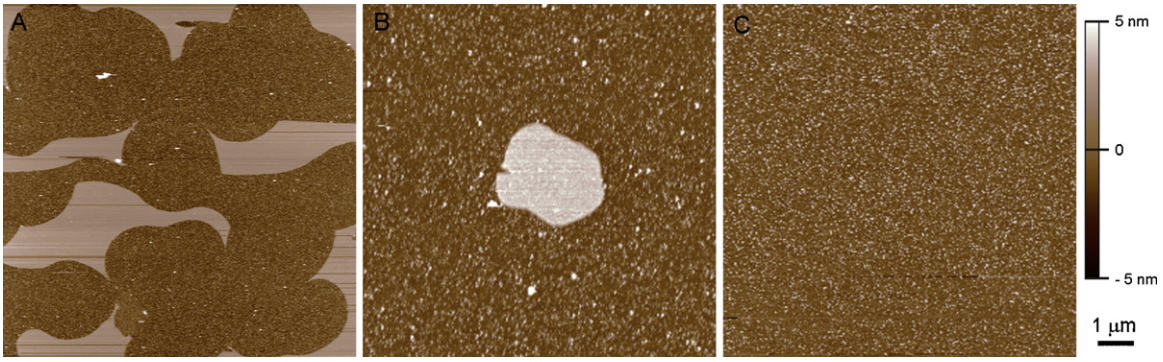

Fig. 6. AFM height images showing the increased rate of bilayer solubilization induced by Aβ monomers ($t = 10$ min) in DOPC bilayers containing increasing fractions of cholesterol. (A) 10 mol%, (B) 25 mol% and (C) 50 mol% cholesterol.

oligomeric Aβ assembly composed of no more than 7 monomers in height above the bilayer surface. EM studies of $A\beta_{1-40}$ morphology show that oligomerization results in the formation of protofibrils with diameters of 5 nm, suggesting that the surface adsorption seen here is that of paranuclei, an end-on assembly of Aβ monomers (Fraser et al., 1992). A previous study of Aβ oligomerization determined that $A\beta_{1-40}$ forms tetrameric paranuclei that assemble to form larger oligomers and protofibrils and our results are consistent with this finding (Bitan et al., 2003). The mechanical strength of the oligomeric assemblies is likely to be increased by an increase in higher order structure, leading to reduced deformation by the AFM tip during imaging (compared to that of monomers). The measured heights of the oligomeric assemblies (4.4 ± 0.4 nm to 5.5 ± 0.5 nm) compared to protofibril diameters of 5 nm determined by EM (Fraser et al., 1992), suggest that the oligomeric assemblies do not penetrate the bilayer beyond the depth of the headgroup region (ca. 1 nm) (Sheikh et al., 2011; Sun et al., 1994).

The formation of protofibrillar oligomers above the Tm of the DPPC bilayer was notable in relation to the known tendency of Aβ to form fibrillar structures in vivo. This suggests that the lipid bilayer needs to be in fluid rather than gel or crystalline phase state in order for the surface-bound Aβ paranuclei to orient in a manner conducive to protofibril formation.

The difference of 1.1 nm between the height (above the surface) of Aβ assemblies formed at 26 °C and 44 °C suggests that an increasing part of the adsorbed protofibrils are incorporated into the headgroup region of the lipid bilayer when the bilayer is in the fluid phase. This is broadly consistent with the predictions of recent molecular dynamics simulations of the interaction of Aβ monomers with DPPC bilayers (Strodel et al., 2010; Davis and Berkowitz, 2009). A previous CD study has shown that increasing the temperature of $A\beta_{1-40}$ peptides from 0 °C to 37 °C results in a reversible change in conformation from random coil to β-strand transition without oligomerization (Gursky and Aleshkov, 2000). Aging (for 12 h) at 37 °C, or increasing the solution temperature to 80 °C, resulted in β-sheet formation and oligomerization. The faster kinetics of the protofibril formation observed here strongly suggest that protofibril formation is induced by Aβ interactions with the fluid phase DPPC bilayer, rather than by the effect of the increased temperature on the Aβ peptides per se.

Incorporation of cholesterol into DPPC bilayers (at a concentration of 33 mol%) had the effect of increasing the initial kinetics of Aβ area coverage on the bilayer surface by two orders of magnitude. The rapid kinetics associated with this increase, suggest that this results from an increase in binding affinity of Aβ monomers for the bilayer containing cholesterol (compared to pure DPPC bilayers). Additionally the formation of these layers into domains may suggest the sequestering of cholesterol in the bilayer domains associated with the Aβ assemblies, although we also saw the formation of small layered assemblies in pure DPPC bilayers, and therefore the observed increase in the initial kinetics of bilayer surface area coverage may be due to a change in the physical properties of the bilayer itself as a results of cholesterol incorporation. Indeed cholesterol is known to broaden the gel-fluid phase transition of phosphatidylcholine bilayers (the 'fluidizing' effect) on phosphatidylcholine bilayers, an effect which is likely to facilitate the increase in binding affinity and kinetics observed at this temperature (Gershfeldt, 1978; Mabrey et al., 1978).

In DPPC bilayers with high (50 mol%) cholesterol we saw reversible insertion of the Aβ assembly into the hydrophobic core of the bilayer triggered by small changes (ca. 50 pN) in imaging force. Such small changes in imaging force would be extremely unlikely to induce such a substantial change in height of the Aβ assembly itself and variation of this magnitude was not observed in the imaging of isolated monomers on mica. This strongly suggests that increasing membrane cholesterol content facilitates Aβ assembly incorporated into the hydrophobic core structure of the bilayer, forming a structure that is less dissipative than the bilayer itself. This is in good agreement with the study by Ji and Wu (2002) who showed that in the presence of cholesterol, Aβ is inserted into the bilayer with an associated increase of approximately 60% in α-helical content.

The formation of defects in DOPC bilayers contrasts with the interaction of monomeric Aβ with DPPC bilayers, where oligomeric assembly formation was observed on the surface of the bilayer. This may be in part related to the higher fluidity of the DOPC bilayer compared to that of the DPPC bilayer, but is highly suggestive of a different mechanism of interaction. In addition, the dimensions and morphology of the globular structures detected are highly suggestive of micelle formation. It is known from structural studies that the $A\beta_{1-40}$ forms an amphiphilic structure and that amphiphilic peptides form micellar structures (Petkova et al., 2002; Zhang, 2003). Indeed Aβ has been shown by SANS to form micelle-like spherocylindrical aggregates of 11 nm length (Yong et al., 2002). Peptides with tendencies to form micellar structures exhibit membrane destabilizing detergent action (Heerklotz and Seelig, 2001). The observed interaction is therefore highly suggestive of bilayer solubilization by micellar Aβ structures. Additionally, we see a significant increase the rate of membrane disruption with increasing bilayer cholesterol content.

Again, the fluidizing effect of cholesterol on phosphatidylcholine bilayers appears to have the same enhancing effect on the affinity of Aβ for unsaturated DOPC bilayers as with saturated DPPC bilayers, despite a difference in the mechanism of interaction.

In cellular studies, it has been shown that both soluble oligomers and insoluble mature fibrils (but not soluble monomers) are neurotoxic (Walsh et al., 1997, 1999, 2002). Additionally, in vivo, neuronal membranes contain fatty acid chains that are predominantly (but

not exclusively) unsaturated, with fatty acid chain lengths mainly between 32 and 40 carbon residues (Takamori et al., 2006). At a physiological temperature of 37 °C, this suggests that cellular saturated lipids will be predominantly in the gel phase and unsaturated lipids predominantly in the fluid phase.

Based on our findings, this would suggest that amyloid Aβ monomers would form layered assemblies on saturated cellular lipid domains in vivo. These assemblies may act as nucleation centers for fibril formation, particularly at lipid domain boundaries. On unsaturated lipid domains, our results suggest that the amyloid Aβ monomers would form membrane defects by lipid solubilization. Although fluid cellular membranes are likely to be self-healing at the low concentrations of amyloid Aβ monomers seen in vivo, exposure to soluble Aβ monomers is likely to result in cell degradation. What is less certain is what happens at domain boundaries and would be an interesting target for future research. Both effects would be enhanced by the relatively high cholesterol concentration of neuronal cells.

These findings suggest that both the mechanism and kinetics of interaction between amyloid Aβ and lipid membranes are highly sensitive to lipid composition, phase state and cholesterol content.

Acknowledgements

This work was supported by Science Foundation Ireland (07/IN.1/B931). J.J.M. acknowledges Science Foundation Ireland Stokes Lectureship for financial support.

Appendix A. Supplementary data

Supplementary data associated with this article can be found, in the online version, at doi:10.1016/j.chemphyslip.2011.11.011.

References

Arispe, N., Pollard, H.B., Rojas, E., 1993a. Giant multilevel cation channels formed by Alzheimer disease amyloid β-protein [AβP(1–40)] in bilayer membranes. Proc. Natl. Acad. Sci. U. S. A. 90, 10573–10577.

Arispe, N., Rojas, E., Pollard, H.B., 1993b. Alzheimer disease amyloid β protein forms calcium channels in bilayer membranes: blockade by tromethamine and aluminum. Proc. Natl. Acad. Sci. U. S. A. 90, 567–571.

Avdulov, N.A., Chochina, S.V., Igbavboa, U., Vassiliev, A.V., Wood, W.G., 1997. Lipid binding to amyloid β-peptide: preferential binding of cholesterol as compared with phosphatidylcholine and fatty acids. J. Neurochem. 69, 1746–1752.

Bhatia, R., Lin, H., Lal, R., 2000. Fresh and globular amyloid β protein (1–42) induces rapid cellular degeneration: evidence for AβP channel-mediated cellular toxicity. FASEB J. 14, 1234–1243.

Bitan, G., Kirkitadze, M.D., Lomakin, A., Vollers, S.S., Benedek, G.B., Teplow, D.B., 2003. Amyloid β-protein (Aβ) assembly: Aβ40 and Aβ42 oligomerize through distinct pathways. Proc. Natl. Acad. Sci. U. S. A. 100, 330–335.

Bodovitz, S., Klein, W.L., 1996. Cholesterol modulates α-secretase cleavage of amyloid precursor protein. J. Biol. Chem. 271, 4436–4440.

Choucair, A., Chakrapani, M., Chakravarthy, B., Katsaras, J., Johnston, L.J., 2007. Preferential accumulation of Aβ(1–42) on gel phase domains of lipid bilayers: an AFM and fluorescence study. BBA-Biomembranes 1768, 146–154.

Cleveland, J.P., Anczykowski, B., Schmid, A.E., Elings, V.B., 1998. Energy dissipation in tapping-mode atomic force microscopy. Appl. Phys. Lett. 72, 2613–2615.

Davis, C.H., Berkowitz, M.L., 2009. Interaction between amyloid-β (1–42) peptide and phospholipid bilayers: a molecular dynamics study. Biophys. J. 96, 785–797.

Demuro, A., Mina, E., Kayed, R., Milton, S.C., Parker, I., Glabe, C.G., 2005. Calcium dysregulation and membrane disruption as a ubiquitous neurotoxic mechanism of soluble amyloid oligomers. J. Biol. Chem. 280, 17294–17300.

Fraser, P.E., Nguyen, J.T., Inouye, H., Surewicz, W.K., Selkoe, D.J., Podlisny, M.B., Kirschner, D.A., 1992. Fibril formation by primate, rodent, and Dutch-hemorrhagic analogues of Alzheimer amyloid betaprotein. Biochemistry 31, 10716–10723.

Gershfeldt, N.-L., 1978. Equilibrium studies of lecithin–cholesterol interactions: I. Stoichiometry of lecithin–cholesterol complexes in bulk systems. Biophys. J. 22, 469–488.

Gursky, O., Aleshkov, S., 2000. Temperature-dependent β-sheet formation in β-amyloid Aβ1–40 peptide in water: uncoupling β-structure folding from aggregation. Biochim. Biophys. Acta 1476, 93–102.

Haass, C., Schlossmacher, M.G., Hung, A.Y., Vigo-Pelfrey, C., Mellon, A., Ostaszewski, B.L., Lieberburg, I., Koo, E.H., Schenk, D., Teplow, D.B., Selkoe, D.J., 1992. Amyloid β-peptide is produced by cultured cells during normal metabolism. Nature 359, 322–325.

Harris, J.R., 2008. Cholesterol binding to amyloid-β fibrils: a TEM study. Micron 39, 1192–1196.

Hartmann, T., Bieger, S.C., Brühl, B., Tienari, P.J., Ida1, N., Allsop, D., Roberts, G.W., Masters, C.L., Dotti, C.G., Unsicker, K., Beyreuther, K., 1997. Distinct sites of intracellular production for Alzheimer's disease Aβ40/42 amyloid peptides. Nat. Med. 3, 1016–1020.

Heerklotz, H., Seelig, J., 2001. Detergent-like action of the antibiotic peptide surfactin on lipid membranes. Biophys. J. 81, 1547–1554.

Irvine, G.B., El-Agnaf, O.M., Shankar, G.M., Walsh, D.M., 2008. Protein aggregation in the brain: the molecular basis for Alzheimer's and Parkinson's diseases. Mol. Med. 14, 451–464.

Ji, S.-R., Wu, Y., Sui, S-f., 2002. Cholesterol is an important factor affecting the membrane insertion of β-amyloid peptide (Aβ1–40), which may potentially inhibit the fibril formation. J. Biol. Chem. 277, 6273–6279.

Kawahara, M., Arispe, N., Kuroda, Y., Rojas, E., 1997. Alzheimer's disease amyloid β protein forms Zn^{2+}-sensitive, cation-selective channels across excised membrane patches from hypothalamic neurons. Biophys. J. 73, 67–75.

Leon, E.J., Verma, N., Zhang, S., Lauffenburger, D.A., Kamm, R.D., 1998. Mechanical properties of a self-assembling oligopeptide matrix. J. Biomater. Sci. Polym. Ed. 9, 297–312.

Lin, H., Zhu, Y.J., Lal, R., 1999. Amyloid β protein (1–40) forms calcium-permeable, Zn^{2+}-sensitive channel in reconstituted lipid vesicles. Biochemistry 38, 11189–11196.

Losic, D., Lisandra, L.M., Aguilar, M.-I., Small, D.H., 2006. β-Amyloid fibril formation is promoted by step edges of highly oriented pyrolytic graphite. Biopolymers (Pept. Sci.) 84, 519–526.

Mabrey, S., Mateo, P.L., Sturtevant, J.M., 1978. High-sensitivity scanning calorimetric study of mixtures of cholesterol with dimyristoyl- and dipalmitoylphosphatidylcholines. Biochemistry 17, 2464–2468.

McLaurin, J., Chakrabartty, A., 1997. Characterization of the interactions of Alzheimer β-amyloid peptides with phospholipid membranes. Eur. J. Biochem. 245, 355–363.

Middleburg, A.P.J., He, L., Dexter, A.F., Shen, H.-H., Holt, S.A., Thomas, R.K., 2008. The interfacial structure and Young's modulus of peptide films having switchable mechanical properties. J. R. Soc. Interface 5, 47–54.

Nag, S., Chen, J., Irudayaraj, J., Maiti, S., 2010. Measurement of the attachment and assembly of small amyloid-β oligomers on live cell membranes at physiological concentrations using single-molecule tools. Biophys. J. 99, 1969–1975.

Petkova, A.T., Ishii, Y., Balbach, J.J., Antzutkin, O.N., Leapman, R.D., Delaglio, F., Tycko, R., 2002. A structural model for Alzheimer's β-amyloid fibrils based on experimental constraints from solid state NMR. Proc. Natl. Acad. Sci. U. S. A. 99, 16742–16747.

Pike, C.J., Burdick, D., Walencewicz, A.J., Glabe, C.G., Cotman, C.W., 1993. Neurodegeneration induced by β-amyloid peptides in vitro: the role of peptide assembly state. J. Neurosci. 13, 1676–1687.

Quist, A., Doudevski, I., Lin, H., Azimova, R., Ng, D., Frangione, B., Kagan, B., Ghiso, J., Lal, R., 2005. Amyloid ion channels: a common structural link for protein-misfolding disease. Proc. Natl. Acad. Sci. U. S. A. 102, 10427–10432.

Rinia, H.A., Kik, R.A., Demel, R.A., Snel, M.M.E., Killian, J.A., van der Eerden, J.P.J.M., de Kruijff, B., 2000. Visualization of highly ordered striated domains induced by transmembrane peptides in supported phosphatidylcholine bilayers. Biochemistry 39, 5852–5858.

Selkoe, D.J., 1991. The molecular pathology of Alzheimer's disease. Neuron 6, 487–498.

Sheikh, K.H., Giordani, C., Kilpatrick, J.I., Jarvis, S.P., 2011. Direct submolecular scale imaging of mesoscale molecular order in supported dipalmitoylphosphatidylcholine bilayers. Langmuir 27, 3749–3753.

Shobab, L.A., Hsiung, G-Y.R., Feldman, H.H., 2005. Cholesterol in Alzheimer's disease. Lancet Neurol. 4, 841–852.

Snyder, S.W., et al., 1994. Amyloid-β aggregation: selective inhibition of aggregation in mixtures of amyloid with different chain lengths. Biophys. J. 67, 1216–1228.

Strodel, B., Lee, J.W.L., Whittleston, C.S., Wales, D.J., 2010. Transmembrane structures for Alzheimer's $A\beta_{1-42}$ oligomers. J. Am. Chem. Soc. 132, 13300–13312.

Sun, W.-J., Suter, R.M., Knewtson, M.A., Worthington, C.R., Tristram-Nagle, S., Zhang, R., Nagle, J.F., 1994. Order and disorder in fully hydrated unoriented bilayers of gel phase dipalmitoylphosphatidylcholine. Phys. Rev. E. 49, 4665–4676.

Takamori, S., et al., 2006. Molecular anatomy of a trafficking organelle. Cell 127, 831–846.

Terzi, E., Holzemann, G., Seelig, J., 1995. Self-association of β-amyloid peptide (1–40) in solution and binding to lipid membranes. J. Mol. Biol. 252, 633–642.

Wahrle, S., Das, P., Nyborg, A.C., McLendon, C., Shoji, M., Kawarabayashi, T., Younkin, L.H., Younkin, S.G., Golde, T.E., 2002. Cholesterol-dependent γ-secretase activity in buoyant cholesterol-rich membrane microdomains. Neurobiol. Dis. 9, 11–23.

Walsh, D.M., Lomakin, A., Benedek, G.B., Condron, M.M., Teplow, D.B., 1997. Amyloid β-protein fibrillogenesis: detection of a protofibrillar intermediate. J. Biol. Chem. 35, 22364–22372.

Walsh, D.M., Hartley, D.M., Kusumoto, Y., Fezoui, Y., Condron, M.M., Lomakin, A., Benedek, G.B., Selkoe, D.J., Teplow, D.B., 1999. Amyloid β-protein fibrillogenesis: structure and biological activity of protofibrillar intermediates. J. Biol. Chem. 36, 25945–25952.

Walsh, D.M., Klubin, I., Fadeeva, J.V., Cullen, W.K., Anwyl, R., Wolfe, M.S., Rowan, M.J., Selkoe, D.J., 2002. Naturally secreted oligomers of amyloid β protein potently inhibit hippocampal long-term potentiation in vivo. Nature 416, 535–539.

Yarrow, F., Vlugt, T.J.H., van der Eerden, J.P.J.M., Snel, M.M.E., 2005. Melting of a DPPC lipid bilayer observed with atomic force microscopy and computer simulation. J. Cryst. Growth 275, el417–el421.
Yip, C.M., McLaurin, J., 2001. Amyloid-β peptide assembly: a critical step in fibrillogenesis and membrane disruption. Biophys. J. 80, 1359–1371.
Yip, C.M., Darabie, A.A., McLaurin, J., 2002. Aβ42-peptide assembly on lipid bilayers. J. Mol. Biol. 318, 97–107.
Yong, W., Lomakin, A., Kirkitadze, M.D., Teplow, D.B., Chen, S.H., Benedek, G.B., 2002. Structure determination of micelle-like intermediates in amyloid β-protein fibril assembly by using small angle neutron scattering. Proc. Natl. Acad. Sci. U. S. A. 99, 150–154.
Zhang, S., 2003. Fabrication of novel biomaterials through molecular self-assembly. Nat. Biotechnol. 21, 1171–1178.